



**HAL**  
open science

## The role of H<sub>2</sub>SO<sub>4</sub>-NH<sub>3</sub> anion clusters in ion-induced aerosol nucleation mechanisms in the boreal forest

Chao Yan, Lubna Dada, Clémence Rose, Tuija Jokinen, Wei Nie, Siegfried Schobesberger, Heikki Junninen, Katrianne Lehtipalo, Nina Sarnela, Ulla Makkonen, et al.

### ► To cite this version:

Chao Yan, Lubna Dada, Clémence Rose, Tuija Jokinen, Wei Nie, et al.. The role of H<sub>2</sub>SO<sub>4</sub>-NH<sub>3</sub> anion clusters in ion-induced aerosol nucleation mechanisms in the boreal forest. *Atmospheric Chemistry and Physics*, 2018, 18 (17), pp.13231 - 13243. 10.5194/acp-18-13231-2018 . hal-01893564

**HAL Id: hal-01893564**

**<https://uca.hal.science/hal-01893564>**

Submitted on 11 Oct 2018

**HAL** is a multi-disciplinary open access archive for the deposit and dissemination of scientific research documents, whether they are published or not. The documents may come from teaching and research institutions in France or abroad, or from public or private research centers.

L'archive ouverte pluridisciplinaire **HAL**, est destinée au dépôt et à la diffusion de documents scientifiques de niveau recherche, publiés ou non, émanant des établissements d'enseignement et de recherche français ou étrangers, des laboratoires publics ou privés.



# The role of H<sub>2</sub>SO<sub>4</sub>-NH<sub>3</sub> anion clusters in ion-induced aerosol nucleation mechanisms in the boreal forest

Chao Yan<sup>1</sup>, Lubna Dada<sup>1</sup>, Clémence Rose<sup>1</sup>, Tuija Jokinen<sup>1</sup>, Wei Nie<sup>1,2</sup>, Siegfried Schobesberger<sup>1,3</sup>, Heikki Junninen<sup>1,4</sup>, Katrianne Lehtipalo<sup>1</sup>, Nina Sarnela<sup>1</sup>, Ulla Makkonen<sup>5</sup>, Olga Garmash<sup>1</sup>, Yonghong Wang<sup>1</sup>, Qiaozhi Zha<sup>1</sup>, Pauli Paasonen<sup>1</sup>, Federico Bianchi<sup>1</sup>, Mikko Sipilä<sup>1</sup>, Mikael Ehn<sup>1</sup>, Tuukka Petäjä<sup>1,2</sup>, Veli-Matti Kerminen<sup>1</sup>, Douglas R. Worsnop<sup>1,6</sup>, and Markku Kulmala<sup>1,2,7</sup>

<sup>1</sup>Institute for Atmospheric and Earth System Research / Physics, Faculty of Science, University of Helsinki, P. O. Box 64, 00014, Helsinki, Finland

<sup>2</sup>Joint International Research Laboratory of Atmospheric and Earth System Sciences, School of Atmospheric Sciences, Nanjing University, Nanjing, 210046, China

<sup>3</sup>Department of Applied Physics, University of Eastern Finland, 70211 Kuopio, Finland

<sup>4</sup>Institute of Physics, University of Tartu, Ülikooli 18, 50090 Tartu, Estonia

<sup>5</sup>Finnish Meteorological Institute, 00560 Helsinki, Finland

<sup>6</sup>Aerodyne Research, Inc., Billerica, MA 01821, USA

<sup>7</sup>Aerosol and Haze Laboratory, Beijing Advanced Innovation Center for Soft Matter Science and Engineering, Beijing University of Chemical Technology, Beijing, 100029, China

**Correspondence:** Chao Yan (chao.yan@helsinki.fi)

Received: 19 February 2018 – Discussion started: 10 April 2018

Revised: 11 August 2018 – Accepted: 22 August 2018 – Published: 13 September 2018

**Abstract.** New particle formation (NPF) provides a large source of atmospheric aerosols, which affect the climate and human health. In recent chamber studies, ion-induced nucleation (IIN) has been discovered as an important pathway of forming particles; however, atmospheric investigation remains incomplete. For this study, we investigated the air anion compositions in the boreal forest in southern Finland for three consecutive springs, with a special focus on H<sub>2</sub>SO<sub>4</sub>-NH<sub>3</sub> anion clusters. We found that the ratio between the concentrations of highly oxygenated organic molecules (HOMs) and H<sub>2</sub>SO<sub>4</sub> controlled the appearance of H<sub>2</sub>SO<sub>4</sub>-NH<sub>3</sub> clusters ( $3 < no.S < 13$ ): all such clusters were observed when  $[HOM]/[H_2SO_4]$  was smaller than 30. The number of H<sub>2</sub>SO<sub>4</sub> molecules in the largest observable cluster correlated with the probability of ion-induced nucleation (IIN) occurrence, which reached almost 100 % when the largest observable cluster contained six or more H<sub>2</sub>SO<sub>4</sub> molecules. During selected cases when the time evolution of H<sub>2</sub>SO<sub>4</sub>-NH<sub>3</sub> clusters could be tracked, the calculated ion growth rates exhibited good agreement across measurement methods and cluster (particle) sizes. In these cases, H<sub>2</sub>SO<sub>4</sub>-

NH<sub>3</sub> clusters alone could explain ion growth up to 3 nm (mobility diameter). IIN events also occurred in the absence of H<sub>2</sub>SO<sub>4</sub>-NH<sub>3</sub>, implying that other NPF mechanisms also prevail at this site, most likely involving HOMs. It seems that H<sub>2</sub>SO<sub>4</sub> and HOMs both affect the occurrence of an IIN event, but their ratio ( $[HOMs]/[H_2SO_4]$ ) defines the primary mechanism of the event. Since that ratio is strongly influenced by solar radiation and temperature, the IIN mechanism ought to vary depending on conditions and seasons.

## 1 Introduction

Atmospheric aerosol particles are known to influence human health and the climate (Heal et al., 2012; Stocker et al., 2013). New particle formation (NPF) from gas-phase precursors contributes to a major fraction of the global cloud condensation nuclei population (Merikanto et al., 2009; Kerminen et al., 2012; Dunne et al., 2016; Gordon et al., 2017) and provides an important source of particulate air pollutants in many urban environments (Guo et al., 2014).

Although NPF is an abundant phenomenon and has been observed in different places around the globe within the boundary layer (Kulmala et al., 2004), the detailed mechanisms at each location may differ and are still largely unknown. Experiments done in the CLOUD chamber (Cosmics Leaving Outside Droplets) at CERN explored different NPF mechanisms on a molecular level, including sulfuric acid (H<sub>2</sub>SO<sub>4</sub>) and ammonia (NH<sub>3</sub>) nucleation (Kirkby et al., 2011), H<sub>2</sub>SO<sub>4</sub> and dimethylamine nucleation (Almeida et al., 2013), and pure biogenic nucleation (Kirkby et al., 2016) from highly oxygenated organic molecules (HOMs) (Ehn et al., 2014). While chamber experiments can mimic some properties of ambient observations (Schobesberger et al., 2013), it is still unclear to what extent these chamber findings can be applied to understand NPF in the more complex atmosphere, mostly due to the challenges in atmospheric measurements and characterization of the nucleating species.

In the aforementioned chamber studies, ions have been shown to play a crucial role in enhancing new particle formation, which is known as ion-induced nucleation (IIN). The importance of IIN varies significantly depending on the temperature as well as the concentration and composition of the ion species. For instance, big H<sub>2</sub>SO<sub>4</sub> ion clusters were not found in the sulfur-rich air mass from Atlanta, suggesting the minor role of IIN (Eisele et al., 2006). Similar conclusions were drawn based on the observations in Boulder (Iida et al., 2006) and Hyytiälä (e.g., Manninen et al., 2010), although the suggested importance of IIN in cold environments, such as upper troposphere, cannot be excluded (Lovejoy et al., 2004; Kürten et al., 2016). Recently, the CLOUD experiments have revealed that the importance of IIN can be negligible in the H<sub>2</sub>SO<sub>4</sub>-dimethylamine system (Almeida et al., 2013), moderate in the H<sub>2</sub>SO<sub>4</sub>-NH<sub>3</sub> system (Kirkby et al., 2011), and dominating in the pure HOMs system (Kirkby et al., 2016). However, it is also important to note that the ion-pair concentration in Hyytiälä is lower than in the CLOUD chamber, which partly explains its smaller contribution of IIN (Wagner et al., 2017).

The recently developed atmospheric-pressure interface time-of-flight mass spectrometer (APi-TOF) (Junninen et al., 2010) has been used for measuring ion composition at the SMEAR II station in Hyytiälä since 2009. Ehn et al. (2010) first showed that the negative ion population varied significantly, with H<sub>2</sub>SO<sub>4</sub> clusters dominating during the day and HOM-NO<sub>3</sub><sup>-</sup> clusters doing so during the night. This variation was further studied by Bianchi et al. (2017), who grouped HOM-containing ions by separating the HOMs into non-nitrate- and nitrate-containing species as well as into ion adducts with HSO<sub>4</sub><sup>-</sup> or NO<sub>3</sub><sup>-</sup>. At nighttime, HOMs may form negatively charged clusters containing up to 40 carbons (Bianchi et al., 2017; Frege et al., 2018). In the daytime, H<sub>2</sub>SO<sub>4</sub> and H<sub>2</sub>SO<sub>4</sub>-NH<sub>3</sub> clusters appear to be the most prominent negative ions (Schobesberger et al., 2015, 2013). However, they have not yet been thoroughly studied regard-

ing their appearance and their plausible links to atmospheric IIN.

Along with the changes in temperature and in ion concentration and composition, the importance of IIN is expected to vary considerably. In this study, we revisit the ion measurement in Hyytiälä, aiming to connect our current understanding of the formation of ion clusters to the significance of IIN, with a special focus on the fate of H<sub>2</sub>SO<sub>4</sub>-NH<sub>3</sub> clusters. We also extend our analysis to ions other than H<sub>2</sub>SO<sub>4</sub> clusters, i.e., HOMs, and identify their role in IIN, in addition to other measured parameters on site. Finally, this study confirms the consistency between chamber findings and atmospheric observations, even though it seems that at least two separate mechanisms alternately control the IIN in Hyytiälä.

## 2 Materials and methods

For this study, we used data collected at the Station for Measuring Forest Ecosystem-Atmospheric Relations (SMEAR II station), in Hyytiälä, southern Finland (Hari and Kulmala, 2005). In this study, our data sets were obtained from intensive campaigns in three consecutive springs (2011–2013). The exact time periods of the APi-TOF measurements are 22 March until 24 May 2011, 31 March until 28 April 2012, and 7 April until 8 June 2013. For 134 days we were able to extend our analysis to include (i) ion composition and chemical characterization using the APi-TOF (Junninen et al., 2010), (ii) particle and ion number size distribution using a neutral cluster and air ion spectrometer (NAIS) (e.g., Mirme and Mirme 2013), (iii) concentrations of H<sub>2</sub>SO<sub>4</sub> and HOMs measured by the chemical-ionization atmospheric-pressure interface time-of-flight mass spectrometer (CI-APi-TOF; see, e.g., Jokinen et al. (2012), Ehn et al. (2014), and Yan et al. (2016)), and (iv) other relevant parameters, e.g., NH<sub>3</sub> (Makkonen et al., 2014), temperature, and cloudiness (Dada et al., 2017).

### 2.1 Measurement of atmospheric ions

The composition of atmospheric anions was measured using the atmospheric-pressure interface time-of-flight mass spectrometer (APi-TOF) (Junninen et al., 2010). The instrument was situated inside a container in the forest, directly sampling the air outside. To minimize the sampling losses, we firstly drew the air at a greater flow rate within a wide tube (40 mm inner diameter), and another 30 cm long coaxial tube (10 mm outer diameter and 8 mm inner diameter) inside the wider one was used to draw 5 L min<sup>-1</sup> towards the APi-TOF, 0.8 L min<sup>-1</sup> of which entered through the pinhole. After entering the pinhole, the ions were focused and guided through two quadrupoles and one ion lens and finally detected by the time-of-flight mass spectrometer.

Unlike the commonly used chemical-ionization mass spectrometer (CIMS), the APi-TOF does not do any ioniza-

tion, so it only measures the naturally charged ions in the sample. In the atmosphere, the ion composition is affected by the proton affinity of the species: molecules with the lowest proton affinity are more likely to lose the proton and thus become negatively charged after colliding many times with other species; similarly, molecules with the highest proton affinity would probably become positively charged ions. In addition to the proton affinity, the neutral concentration also plays a role in determining the ion composition by affecting the collision frequency. Due to the limited ionization rate in the atmosphere, there is always a competition between different species in taking the charges. For example, H<sub>2</sub>SO<sub>4</sub> often dominates the spectrum in the daytime when it is abundant, while at nighttime nitrate ions and their cluster with HOMs are always prominent due to the low chances of colliding with the H<sub>2</sub>SO<sub>4</sub>. Since the signal strength of an ion in the APi-TOF depends not only on the abundance of the respective neutral molecules but also on the availability of other charge-competing species, it is very important to note that the APi-TOF cannot quantify the neutral species.

One important virtue of APi-TOF is that it does not introduce extra energy during sampling, which ensures the sample is least affected when compared to other measurement techniques such as CIMS although fragmentation cannot be fully avoided inside the instrument (Schobesberger et al., 2013). Because of this, it is a well-suited instrument to directly measure the composition of weakly bonded clusters in the atmosphere.

The APi-TOF data were processed with the tofTools package (version 6.08) (Junninen et al., 2010). Since the ion signal in APi-TOF is usually weak, a 5 h integration time was used, after which the signals of H<sub>2</sub>SO<sub>4</sub>-NH<sub>3</sub> clusters and HOMs were fitted (see Fig. 1). For HOM signals, we used the same peaks reported in Bianchi et al. (2017), and the total signal of HOM ions is the sum of all identified HOMs.

It should also be mentioned that the voltage tuning of the instrument was not the same in the years we analyzed, which led to differences in the ion transmission efficiency function. For example, we noticed that in 2011, the largest H<sub>2</sub>SO<sub>4</sub>-NH<sub>3</sub> clusters contained 6 H<sub>2</sub>SO<sub>4</sub> molecules, whereas more than 10 H<sub>2</sub>SO<sub>4</sub> were observed in the clusters in other years. This was very likely due to the very low ion transmission in the mass range larger than about 700 Th for the measurements in 2011. However, this should not affect our results and conclusions because clusters consisting of six H<sub>2</sub>SO<sub>4</sub> molecules had little difference from larger clusters in affecting the IIN in terms of occurrence probability (see more details in Sect. 3.3.1).

## 2.2 Measurement of H<sub>2</sub>SO<sub>4</sub> and HOMs

The concentrations of H<sub>2</sub>SO<sub>4</sub> and HOMs were measured by the chemical-ionization atmospheric-pressure interface time-of-flight mass spectrometer (CI-APi-TOF). The details of the quantification method for H<sub>2</sub>SO<sub>4</sub> can be found in Jokinen et

al. (2012) and those for HOMs in Kirkby et al., 2016. For all data, we applied the same calibration coefficient ( $1.89 \times 10^{10} \text{ cm}^{-3}$ ) reported by Jokinen et al. (2012).

Although the tuning of the CI-APi-TOF was not exactly the same during the measurement period included in this study, no systematic difference was found in the concentrations of H<sub>2</sub>SO<sub>4</sub> and HOMs from different years.

## 2.3 Measurements of ion and particle size distribution

The mobility distribution of charged particles and air ions in the range  $3.2\text{--}0.0013 \text{ cm}^2 \text{ V}^{-1} \text{ s}^{-1}$  (corresponding to mobility diameter 0.8–42 nm) were measured together with the size distribution of total particles in the range  $\sim 2.5\text{--}42 \text{ nm}$  using a NAIS (Airel Ltd.; Mirme and Mirme, 2013). The instrument has two identical differential mobility analyzers (DMAs) which allow for the simultaneous monitoring of positive and negative ions. In order to minimize the diffusion losses in the sampling lines, each analyzer has a sample flow rate of  $30 \text{ L min}^{-1}$  and a sheath flow rate of  $60 \text{ L min}^{-1}$ . In “particle mode”, when measuring total particle concentration, neutral particles are charged by ions produced from a corona discharge in a “pre-charging” unit before they are detected in the DMAs. The charging ions used in this process were previously reported to influence the total particle concentrations below  $\sim 2 \text{ nm}$  (Asmi et al., 2008; Manninen et al., 2010); for that reason, only the particle concentrations above 2.5 nm were used in the present work. Also, each measurement cycle, i.e., 2 min in ion mode and 2 min in particle mode, is followed by an offset measurement, during which the background signal of the instrument is determined and then subtracted from measured ion and particle concentrations. In addition, particle size distributions between 3 and 990 nm were measured with a differential mobility particle sizer (DMPS) described in detail in Aalto et al. (2001). Based on earlier work by Kulmala et al. (2001), these data were used to calculate the condensation sink (CS), which represents the rate of loss of condensing vapors on preexisting particles.

## 2.4 Measurement of the meteorological parameter

The meteorological variables used as supporting data in the present work were measured on a mast, all with a time resolution of 1 min. Temperature and relative humidity were measured at 16.8 m using a PT-100 sensor and relative humidity sensors (Rotronic Hygromet MP102H with Hygroclip HC2-S3, Rotronic AG, Bassersdorf, Switzerland), respectively. Global radiation was measured at 18 m with a pyranometer (Middleton Solar SK08, Middleton Solar, Yarraville, Australia) and further used to calculate the cloudiness parameter, as done previously by Dada et al. (2017, and references therein). This parameter is defined as the ratio of measured global radiation to theoretical global irradiance so that parameter values  $< 0.3$  correspond to a complete cloud

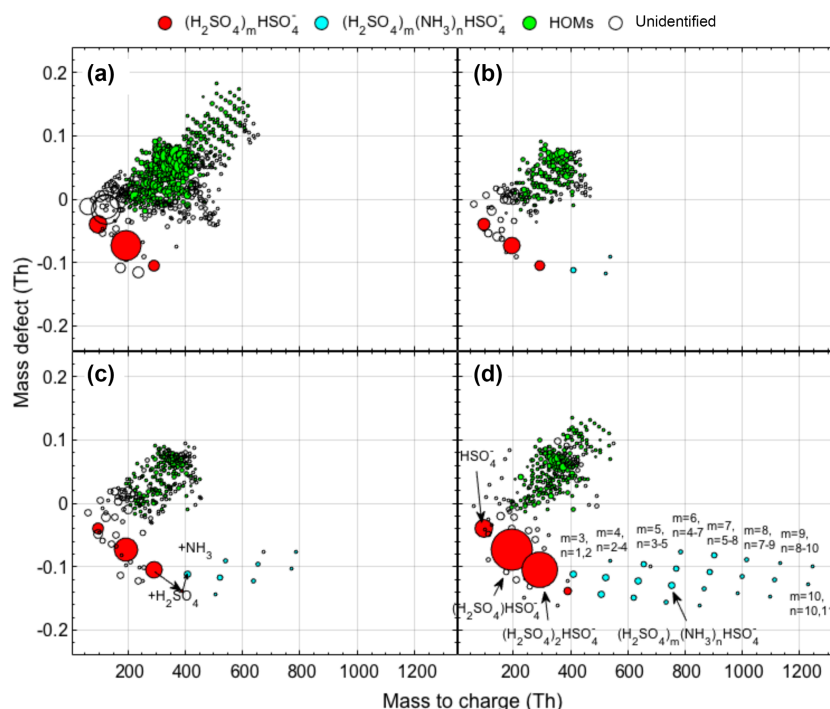


**Figure 1.** Mass defect plot showing the composition of ion clusters on four separate days. (a) NH<sub>3</sub>-free clusters; (b, c, d) H<sub>2</sub>SO<sub>4</sub>-NH<sub>3</sub> clusters with different maximum number of H<sub>2</sub>SO<sub>4</sub> molecules. The circle size is linearly proportional to the logarithm of the signal intensity.

coverage, while values  $> 0.7$  are representative of clear-sky conditions.

## 2.5 Calculation of particle formation rates and growth rates

The formation rate of 2.5 nm particles includes both neutral and charged particles, and it was calculated from the following equation:

$$J_{2.5} = \frac{dN_{2.5-3.5}}{dt} + \text{Coag}S_{2.5} \times N_{2.5-3.5} + \frac{1}{1 \text{ nm}} \text{GR}_{1.5-3} \times N_{2.5-3.5}, \quad (1)$$

where  $N_{2.5-3.5}$  is the particle concentration between 2.5 and 3.5 nm measured with the NAIS in particle mode,  $\text{Coag}S_{2.5}$  is the coagulation sink of 2.5 nm particles, as derived from DMPS measurements, and  $\text{GR}_{1.5-3}$  is the particle growth rate calculated from NAIS measurements in ion mode. Calculating the formation rate of 2.5 nm ions or charged particles includes two additional terms to account for the loss of 2.5–3.5 nm ions due to their recombination with sub –3.5 nm ions of the opposite polarity (fourth term of Eq. 2) and the gain of ions caused by the attachment of sub –2.5 nm ions on 2.5–3.5 nm neutral clusters (fifth term of Eq. 2):

$$J_{2.5}^{\pm} = \frac{dN_{2.5-3.5}^{\pm}}{dt} + \text{Coag}S_{2.5} \times N_{2.5-3.5}^{\pm} + \frac{1}{1 \text{ nm}} \text{GR}_{1.5-3} \times N_{2.5-3.5}^{\pm} + \alpha \times N_{2.5-3.5}^{\pm} N_{<3.5}^{\mp} - \beta \times N_{2.5-3.5} N_{<2.5}^{\pm}, \quad (2)$$

where  $N_{2.5-3.5}^{\pm}$  is the concentration of positive or negative ions between 2.5 and 3.5 nm,  $N_{<2.5}^{\pm}$  is the concentration of sub –2.5 nm ions of the same polarity, and  $N_{<3.5}^{\mp}$  is the concentration of sub –3.5 nm ions of the opposite polarity, all measured with the NAIS in ion mode;  $\alpha$  and  $\beta$  are the ion–ion recombination and the ion–neutral attachment coefficients, respectively, and were assumed to be equal to  $1.6 \times 10^{-6} \text{ cm}^3 \text{ s}^{-1}$  and  $0.01 \times 10^{-6} \text{ cm}^3 \text{ s}^{-1}$ , respectively. We consider these values to be reasonable approximations, keeping in mind that the exact values of both  $\alpha$  and  $\beta$  depend on a number of variables, including the ambient temperature, pressure, and relative humidity as well as the sizes of the colliding objects (ion–ion or ion–aerosol particle) (e.g., Hoppel, 1985; Tamm et al., 2005; Franchin et al., 2015).

$\text{GR}_{1.5-3}$  were calculated from NAIS data in ion mode using the “maximum” method introduced by (Hirsikko et al., 2005). Briefly, the peaking time of the ion concentration in each size bin of the selected diameter range was first determined by fitting a Gaussian to the concentration. The growth rate was then determined by a linear least square fit through the times. The uncertainty in the peak time determination

was reported as the Gaussian's mean 67 % confidence interval and was further taken into account in the growth rate determination.

A similar approach was used to estimate the early growth rate of the H<sub>2</sub>SO<sub>4</sub>-NH<sub>3</sub> clusters detected with the API-TOF. Prior to growth rate calculation, we first converted cluster masses into diameters in order to get growth rate values in nm h<sup>-1</sup> instead of amu h<sup>-1</sup>. For that purpose, we applied the conversion from Ehn et al. (2011), using a cluster density of 1840 kg m<sup>-3</sup>. The time series of the cluster signals were then analyzed in the same way as ion or particle concentrations using the maximum method from Hirsikko et al. (2005), and the growth rate was calculated using the procedure outlined above. Our ability to determine the early cluster growth rate from API-TOF measurements was strongly dependent on the strength of the signal of the different H<sub>2</sub>SO<sub>4</sub>-NH<sub>3</sub> clusters. As a consequence, the reported growth rates characterize a size range which might vary slightly between the events, falling in a range between 1 and 1.7 nm.

### 3 Results and discussion

#### 3.1 Daytime ion composition

We examined the daytime ion composition of 134 days from three consecutive springs (2011–2013) in Hyytiälä. Consistent with the findings by previous studies showing that H<sub>2</sub>SO<sub>4</sub> clusters are the most abundant ions in the daytime (Ehn et al., 2010; Bianchi et al., 2017), we found that NH<sub>3</sub>-free H<sub>2</sub>SO<sub>4</sub> clusters can contain up to three H<sub>2</sub>SO<sub>4</sub> molecules when counting the HSO<sub>4</sub><sup>-</sup> also as one H<sub>2</sub>SO<sub>4</sub> molecule ((H<sub>2</sub>SO<sub>4</sub>)<sub>2</sub>HSO<sub>4</sub><sup>-</sup>) and that NH<sub>3</sub> is always present in clusters containing four or more H<sub>2</sub>SO<sub>4</sub> molecules. The latter feature suggests the important role of NH<sub>3</sub> as a stabilizer in growing H<sub>2</sub>SO<sub>4</sub> clusters (Kirkby et al., 2011). NH<sub>3</sub>-free clusters (at least dimers H<sub>2</sub>SO<sub>4</sub>HSO<sub>4</sub><sup>-</sup>) were observed on 116 measurement days, but the signal intensity varied from day to day. Bigger clusters that contained NH<sub>3</sub> were observed on 39 days, containing a maximum of 4 to 13 H<sub>2</sub>SO<sub>4</sub> per cluster. Figure 1 provides four examples of daytime ion spectra, including an NH<sub>3</sub>-free case (Fig. 1a) and three cases with a different maximum size of H<sub>2</sub>SO<sub>4</sub>-NH<sub>3</sub> clusters (Fig. 1b–d), illustrating the significant variations in signal and maximum size of H<sub>2</sub>SO<sub>4</sub>-NH<sub>3</sub> clusters. In the NH<sub>3</sub>-free case, a larger number of HOM clusters (green circles) was observed, indicating a competition between H<sub>2</sub>SO<sub>4</sub> and HOMs in taking the charges. The largest detected cluster during the measurement was (H<sub>2</sub>SO<sub>4</sub>)<sub>12</sub>(NH<sub>3</sub>)<sub>13</sub>HSO<sub>4</sub><sup>-</sup>, which corresponds to a mobility-equivalent diameter of about 1.7 nm according to the conversion method (Ehn et al., 2011) and is big enough to be detected by particle counters. Since the observed formation of such large H<sub>2</sub>SO<sub>4</sub>-NH<sub>3</sub> clusters is essentially the initial step of IIN, we anticipate that the variation in H<sub>2</sub>SO<sub>4</sub>-NH<sub>3</sub> clusters will influence the occurrence of IIN.

#### 3.2 The determining parameters for H<sub>2</sub>SO<sub>4</sub>-NH<sub>3</sub> cluster formation

To find out the dominating parameters that affect the formation of H<sub>2</sub>SO<sub>4</sub>-NH<sub>3</sub> clusters, we performed a correlation analysis that included the ambient temperature, relative humidity (RH), wind speed, wind direction, CS, and the gas-phase concentrations of NH<sub>3</sub>, H<sub>2</sub>SO<sub>4</sub>, and HOMs. Among all the examined parameters, we found that the ratio between concentrations of HOMs and H<sub>2</sub>SO<sub>4</sub> had the most pronounced influence on the appearance of H<sub>2</sub>SO<sub>4</sub>-NH<sub>3</sub> clusters. As shown in Fig. 2, all H<sub>2</sub>SO<sub>4</sub>-NH<sub>3</sub> clusters were detected when [HOMs] / [H<sub>2</sub>SO<sub>4</sub>] was smaller than 30. No such dependence was observed for only [HOMs] or [H<sub>2</sub>SO<sub>4</sub>]. This implies that the appearance of H<sub>2</sub>SO<sub>4</sub>-NH<sub>3</sub> clusters is primarily controlled by the competition between H<sub>2</sub>SO<sub>4</sub> and HOMs in getting the charges. More specifically, HSO<sub>4</sub><sup>-</sup>, the main charge carrier in the daytime, may either collide with neutral H<sub>2</sub>SO<sub>4</sub> to form large clusters to accommodate NH<sub>3</sub> or collide with HOMs, which prevents the former process. In addition, a reasonable correlation was found between [HOMs] / [H<sub>2</sub>SO<sub>4</sub>] and temperature, likely explained by the emission of volatile organic compounds (VOCs) increasing with temperature, leading to higher HOMs concentrations, whereas the formation of H<sub>2</sub>SO<sub>4</sub> is not strongly temperature-dependent. This observation indicates that the formation of H<sub>2</sub>SO<sub>4</sub>-NH<sub>3</sub> clusters may vary seasonally: we expect to see them more often in cold seasons when HOM concentrations are low and less often in warm seasons.

Parameters other than [HOMs] / [H<sub>2</sub>SO<sub>4</sub>] and temperature seemed to have little influence on the formation of H<sub>2</sub>SO<sub>4</sub>-NH<sub>3</sub> clusters. Interestingly, we found that NH<sub>3</sub> was even lower when H<sub>2</sub>SO<sub>4</sub>-NH<sub>3</sub> clusters were observed, indicating that the NH<sub>3</sub> concentration is not the limiting factor for forming H<sub>2</sub>SO<sub>4</sub>-NH<sub>3</sub> clusters (also see Sect. 3.4). In addition, H<sub>2</sub>SO<sub>4</sub>-NH<sub>3</sub> clusters were observed in a wide range of RH spanning from 20 % to 90 %, suggesting that RH does not affect the cluster formation. Besides, no clear influence from CS, wind speed, or wind direction was observed.

#### 3.3 The relation between H<sub>2</sub>SO<sub>4</sub>-NH<sub>3</sub> clusters and IIN

##### 3.3.1 The effect of cluster size on the probability of IIN events

We identified IIN events using data from the NAIS (ion mode) by observing an increase in the concentration of sub-2 nm ions (Rose et al., 2018) and classified 67 IIN events out of the 134 days of measurements. We defined the IIN probability as the number of days when IIN events were identified out of the total number of days that were counted. For example, the overall IIN probably is 50 % (67 out of 134 days). We found that the maximum observed size of H<sub>2</sub>SO<sub>4</sub>-NH<sub>3</sub> clusters may affect the occurrence of IIN. Our conclusion is complementary to previous theories which stated that the critical

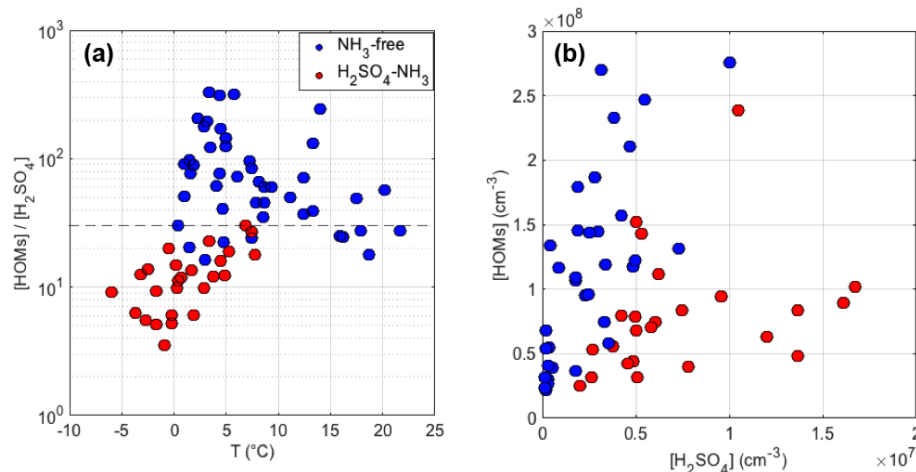


**Figure 2.** The effect of the concentration of HOMs, H<sub>2</sub>SO<sub>4</sub>, their ratio ( $[HOM] / [H_2SO_4]$ ), and temperature on the appearance of H<sub>2</sub>SO<sub>4</sub>-NH<sub>3</sub> clusters.

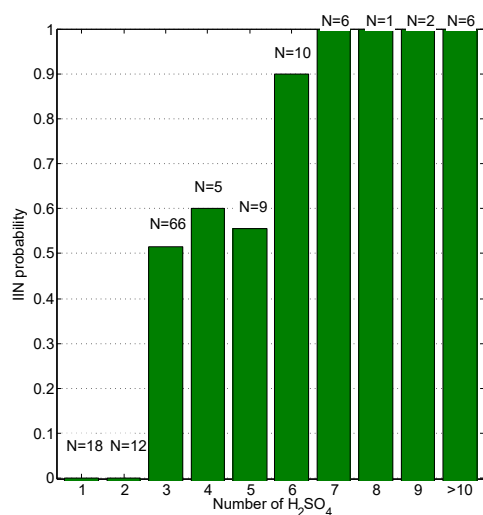


**Figure 3.** The maximum number of H<sub>2</sub>SO<sub>4</sub> molecules observed in clusters and the respective IIN probability. The days when it was unclear if IIN occurred was counted as nonevent days. *N* denotes the number of days when such clusters were the largest observed.

step of particle nucleation is the formation of initial clusters that are big enough for condensational growth to outcompete evaporation (Kulmala et al., 2013). To further understand the size dependency of IIN probability, we investigated the IIN probability when different maximum sizes of H<sub>2</sub>SO<sub>4</sub>-NH<sub>3</sub> clusters were observed. As illustrated in Fig. 3, the IIN probability increases dramatically when larger H<sub>2</sub>SO<sub>4</sub>-NH<sub>3</sub> clusters were observed: IIN events were never observed when only HSO<sub>4</sub><sup>-</sup> or H<sub>2</sub>SO<sub>4</sub>HSO<sub>4</sub><sup>-</sup> were present, whereas the IIN probability increased to about 50%–60% when the largest clusters contained three to five H<sub>2</sub>SO<sub>4</sub> molecules. IIN occurred in 24 out of 25 days (96%) when the largest clusters consisted of no less than six H<sub>2</sub>SO<sub>4</sub> molecules. Thus, it is ev-

ident that the occurrence of IIN is related to the size and thus the stability of H<sub>2</sub>SO<sub>4</sub>-NH<sub>3</sub> clusters and that a cluster consisting of six H<sub>2</sub>SO<sub>4</sub> molecules seems to lie on the threshold size of triggering nucleation.

### 3.3.2 Continuous growth from clusters to 3 nm particles

Although the strong connection between the size of H<sub>2</sub>SO<sub>4</sub>-NH<sub>3</sub> clusters and the occurrence of IIN was confirmed, it is challenging to directly observe the growth of these clusters in the atmosphere, limited by the inhomogeneity of the ambient air and low concentrations of atmospheric ions. Combining APi-TOF and NAIS measurements, we were able to follow the very first steps of the cluster growth for eight of the detected events. In Fig. 4a and b, we present two examples in which the continuous growth of H<sub>2</sub>SO<sub>4</sub>-NH<sub>3</sub> clusters to 3 nm (mobility diameter) particles was directly evaluated using the maximum-time method. The maximum times, determined from APi-TOF and NAIS data independently, fall nicely into the same linear fit. The continuity of the growth and the linearity of the fit suggests that the current mechanism (H<sub>2</sub>SO<sub>4</sub>-NH<sub>3</sub>, acid–base) explains the formation and growth of sub-3 nm ion clusters in these cases. In most cases, the calculation of cluster GR from APi-TOF measurement suffered from large uncertainties, but a weak positive correlation can be observed between the cluster growth rate and H<sub>2</sub>SO<sub>4</sub> concentration (Fig. 4c). This correlation is likely due to the collision of H<sub>2</sub>SO<sub>4</sub> with existing H<sub>2</sub>SO<sub>4</sub>-NH<sub>3</sub> clusters being the limiting step for cluster growth when NH<sub>3</sub> is abundant enough to follow up immediately (Schobesberger et al., 2015).

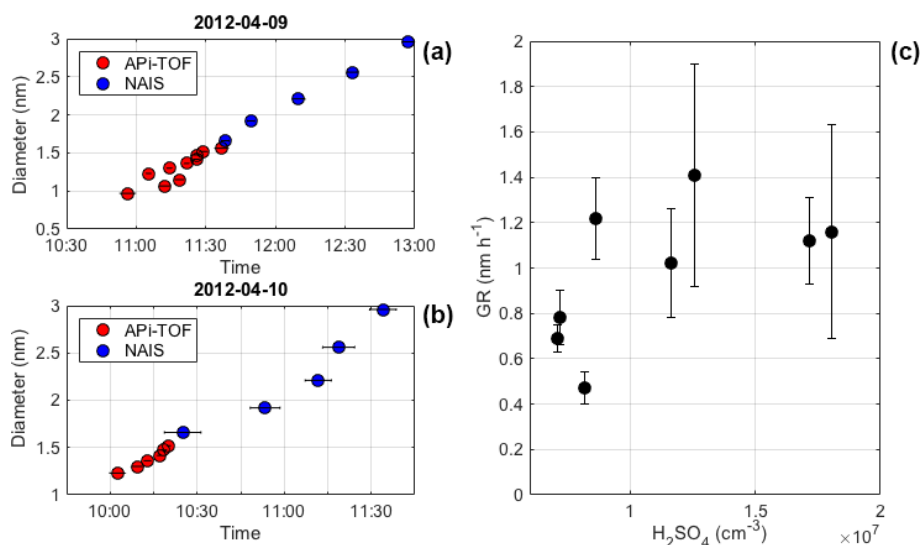


**Figure 4.** Cluster growth rate determined from API-TOF (a) and NAIS (b) measurements using the maximum-time method; the correlation between growth rates and concentrations of H<sub>2</sub>SO<sub>4</sub> molecules (c).

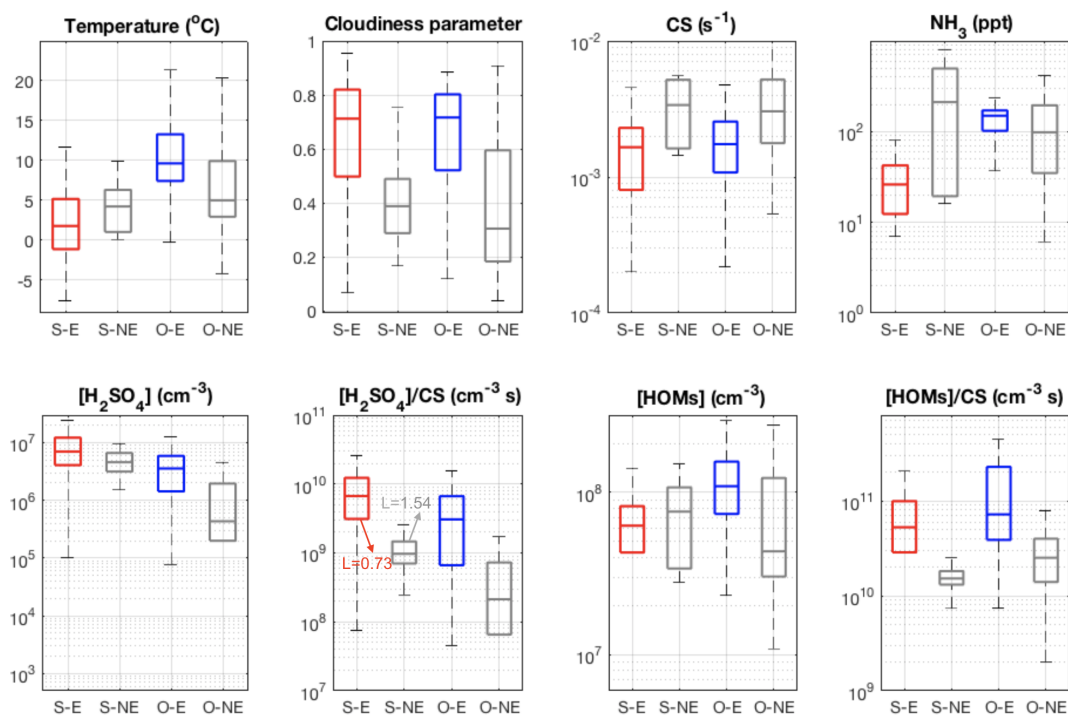


**Figure 5.** Comparison of different parameters for H<sub>2</sub>SO<sub>4</sub>-NH<sub>3</sub>-involved events (S-E, red bars), nonevents with the presence of H<sub>2</sub>SO<sub>4</sub>-NH<sub>3</sub> clusters (S-NE, first column of black bars), other events (O-E, blue bars), and other nonevents (O-NE, second column of black bars).

### 3.4 Evidence for other IIN mechanisms

For the 134 days of measurements, we were able to identify 67 IIN events using the NAIS data, out of which H<sub>2</sub>SO<sub>4</sub>-NH<sub>3</sub> clusters were observed on 32 days, implying that at least 35 IIN events were likely driven by mechanism(s) other

than H<sub>2</sub>SO<sub>4</sub>-NH<sub>3</sub>. In Fig. 5, we classified the days according to the types of IIN observation: 32 IIN events involving H<sub>2</sub>SO<sub>4</sub>-NH<sub>3</sub> (S-E), 3 nonevents with the presence of H<sub>2</sub>SO<sub>4</sub>-NH<sub>3</sub> clusters (S-NE), 35 IIN events involving other mechanisms (O-E), 41 other nonevent days (O-NE), and 23 days with unclear types. We further present the respective

statistics of additional measurements for the first four types of days, including the concentrations of plausible precursor vapors, condensation sinks, and meteorological parameters. It should be noted that the S-NE has only three days; thus, the statistics on this type of day might not be fully representative.

Consistent with the previous discussion (Fig. 2), low temperatures are conducive to IIN events via the H<sub>2</sub>SO<sub>4</sub>-NH<sub>3</sub> mechanism whilst being the highest other type of events (O-E) (Fig. 5a). The clear-sky parameter (100 % – clear sky; 0 % – cloudiness) shows a noticeably higher value during both event types compared to the nonevent cases (Fig. 5b), indicating that photochemistry-related processes are important for all events. Moreover, the CS is obviously lower for both types of events than on nonevent days (Fig. 5c). Although a strong effect of CS on the appearance of H<sub>2</sub>SO<sub>4</sub>-NH<sub>3</sub> clusters has not been noticed, it is a most important parameter in regulating the occurrence of IIN. Similar effects of cloudiness and CS on governing the occurrence of NPF have been reported by Dada et al. (2017) based on long-term data sets.

Remarkably, NH<sub>3</sub> has very low concentrations during H<sub>2</sub>SO<sub>4</sub>-NH<sub>3</sub> events in comparison to the other type of events (Fig. 5d). This is likely due to high NH<sub>3</sub> concentrations coinciding with higher temperature and thus elevated HOMs concentration or the lower stability of H<sub>2</sub>SO<sub>4</sub>-NH<sub>3</sub> clusters at high temperatures that can evaporate NH<sub>3</sub> back to the atmosphere. This observation rules out the addition of NH<sub>3</sub> as a limiting step in the H<sub>2</sub>SO<sub>4</sub>-NH<sub>3</sub> nucleation mechanism, but the participation of NH<sub>3</sub> in the other type of events cannot be excluded.

H<sub>2</sub>SO<sub>4</sub> has the highest concentrations during the H<sub>2</sub>SO<sub>4</sub>-NH<sub>3</sub>-involved events (Fig. 5e), but the concentration of H<sub>2</sub>SO<sub>4</sub> in S-NE days is not much lower, suggesting that the occurrence of H<sub>2</sub>SO<sub>4</sub>-NH<sub>3</sub>-involved events is not solely controlled by the H<sub>2</sub>SO<sub>4</sub> concentration. The incorporating the effect of CS ([H<sub>2</sub>SO<sub>4</sub>]/CS) significantly improves the separation (Fig. 5f). McMurry and colleagues (McMurry et al., 2005) introduced a parameter  $L$  (Eq. 3) to quantitatively evaluate the likelihood of NPF, and they found that NPF mostly occurred when  $L$  is smaller than 1. A similar result has been reported by Kuang et al. (2010), and a slightly different threshold  $L$  value of 0.7 was determined.

$$L = \frac{\text{CS}}{[\text{H}_2\text{SO}_4]} \times \frac{1}{\beta_{11}} \quad (3)$$

Here,  $L$  is a dimensionless parameter representing the probability that NPF will not occur, and  $\beta_{11}$  is the collision rate between H<sub>2</sub>SO<sub>4</sub> vapor molecules, which is characterized as  $4.4 \times 10^{-10} \text{ cm}^3 \text{ s}^{-1}$ . Our results suggest a consistent  $L$  that most (75 percentile) S-E cases happen when  $L$  is lower than 0.73 and most (75 percentile) S-NE cases are observed when  $L$  is larger than 1.54.

HOM concentrations are highest in the case of other events, revealing that HOMs play a key role in this mechanism (Fig. 5f), although the contribution of H<sub>2</sub>SO<sub>4</sub> in this

HOM-involving IIN mechanism cannot be excluded. Similar to the H<sub>2</sub>SO<sub>4</sub>-NH<sub>3</sub>-driven cases, incorporating the CS better distinguishes the event and nonevent cases.

Overall, our results suggest that the concentrations of H<sub>2</sub>SO<sub>4</sub> and HOMs, together with the CS, govern the occurrence of IIN, whereas their ratio determines the exact underlying mechanism (Fig. 2). Although H<sub>2</sub>SO<sub>4</sub>-NH<sub>3</sub> and HOMs clearly drives the S-E and O-E events, respectively, we cannot exclude the later participation of HOMs in S-E cases or H<sub>2</sub>SO<sub>4</sub> in O-E cases. Different NPF mechanisms have also been identified at the Jungfraujoch station (Bianchi et al., 2016; Frege et al., 2018) when influenced by different air masses. At the SMEAR II station, on the other hand, our results suggest that the natural variation in temperature is already sufficient to modify the NPF mechanism by modulating the biogenic VOC emissions.

### 3.5 Contribution of IIN to total nucleation rate

In order to obtain further insight into the importance of IIN during our measurements, we compared the formation rate of 2.5 nm ions,  $J_{\text{ION}} = J_{2.5}^{\pm}$  (see Eq. 2), to the total formation rate of 2.5 nm particles,  $J_{\text{TOT}} = J_{2.5}$  (see Eq. 1). The ratio  $J_{\text{ION}}/J_{\text{TOT}}$  is equal to the charged fraction of the 2.5 nm particle formation rate. In analyzing field measurements, a similar ratio at a certain particle size (typically 2 nm) has commonly been used to estimate the contribution of ion-induced nucleation to the total nucleation rate (see Hirsikko et al., 2011, and references therein). It should be noted that  $J_{\text{ION}}/J_{\text{TOT}}$  represents only a lower limit for the contribution of ion-induced nucleation, as this ratio does not take into account the potential neutralization of growing charged sub-2.5 nm particles by ion-ion recombination (e.g., Kontkanen et al., 2013; Wagner et al., 2017). At present, measuring the true contribution of ion-induced nucleation to the total nucleation rate is possible only in the CLOUD chamber (Wagner et al., 2017).

We were able to calculate  $J_{\text{ION}}$  and  $J_{\text{TOT}}$  for 57 (out of 67) cases, and the ratio  $J_{\text{ION}}/J_{\text{TOT}}$  varied from 4 to 45 %, showing a clear correlation with the HOM signal (Fig. 6a). This indicates the participation of HOMs even in H<sub>2</sub>SO<sub>4</sub>-NH<sub>3</sub>-driven cases. In addition, most of the high  $J_{\text{ION}}/J_{\text{TOT}}$  ratios were observed at moderate or low H<sub>2</sub>SO<sub>4</sub> concentrations; e.g.,  $J_{\text{ION}}/J_{\text{TOT}} > 15 \%$  was only observed when  $[\text{H}_2\text{SO}_4] < 6 \times 10^6 \text{ cm}^{-3}$ . These observations indicate that HOMs are important in high  $J_{\text{ION}}/J_{\text{TOT}}$  cases, while during events driven by H<sub>2</sub>SO<sub>4</sub>-NH<sub>3</sub> clusters, low  $J_{\text{ION}}/J_{\text{TOT}}$  is more often observed. Accordingly, the median value of  $J_{\text{ION}}/J_{\text{TOT}}$  for the H<sub>2</sub>SO<sub>4</sub>-NH<sub>3</sub> cases is about 12 % and is clearly higher (18 %) in HOM-driven events (Fig. 6d). Figures 6b and c reveal that both  $J_{\text{ION}}$  and  $J_{\text{TOT}}$  values are in fact higher in H<sub>2</sub>SO<sub>4</sub>-NH<sub>3</sub> cases, but the neutral nucleation pathway is relatively more enhanced, leading to the lower ratio. These results suggest that ion-induced nucleation plays a more important role in the events driven by HOMs than in

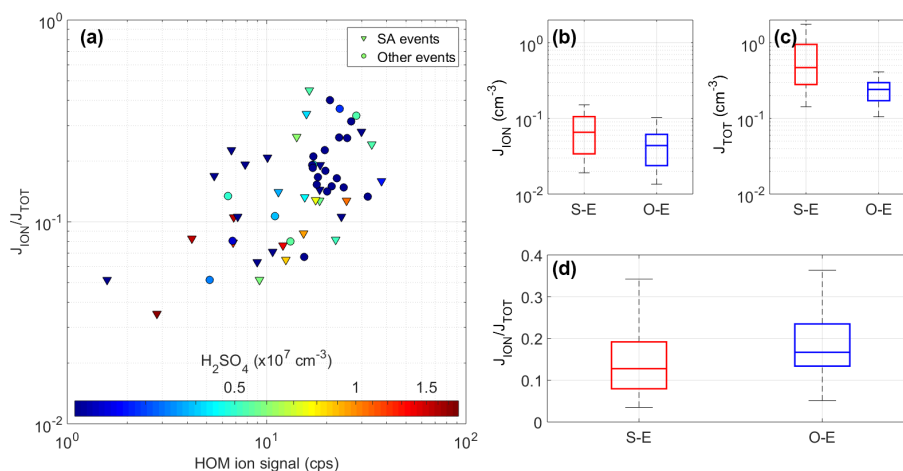


**Figure 6.** Formation rate 2.5 nm ions and total particles (both ions and neutral clusters) under different nucleation mechanisms. (a) Charged fraction of the formation rate of 2.5 nm particles as a function of the total signal of HOM ions color-coded by the H<sub>2</sub>SO<sub>4</sub> concentration, and (b, c, d) the differences in  $J_{\text{ION}}$ ,  $J_{\text{TOT}}$ , and  $J_{\text{ION}}/J_{\text{TOT}}$  between the H<sub>2</sub>SO<sub>4</sub>-NH<sub>3</sub>-involved events (S-E) and other events (O-E).

the events driven by H<sub>2</sub>SO<sub>4</sub>-NH<sub>3</sub>. A plausible explanation is that NH<sub>3</sub> performs well in stabilizing H<sub>2</sub>SO<sub>4</sub> molecules during the clustering process, whereas ions are a relatively more important stabilizing agent for HOM clustering.

#### 4 Summary

We investigated the formation of H<sub>2</sub>SO<sub>4</sub>-NH<sub>3</sub> anion clusters measured by APi-TOF during three springs from 2011 to 2013 in a boreal forest in southern Finland and their connection to IIN. The abundance and maximum size of H<sub>2</sub>SO<sub>4</sub>-NH<sub>3</sub> clusters showed great variability. Out of the total 134 measurement days, H<sub>2</sub>SO<sub>4</sub>-NH<sub>3</sub> clusters were only seen during 39 days. The appearance of these clusters was mainly regulated by the concentration ratio between HOMs and H<sub>2</sub>SO<sub>4</sub>, which can be changed by temperature by modulating the HOM production.

We found that the maximum observable size of H<sub>2</sub>SO<sub>4</sub>-NH<sub>3</sub> clusters has a strong influence on the probability of an IIN event to occur. More specifically, when clusters containing six or more H<sub>2</sub>SO<sub>4</sub> molecules were detected, IIN was observed at almost 100% probability. We further compared the cluster ion growth rates from APi-TOF and NAIS using the maximum-time method. In these H<sub>2</sub>SO<sub>4</sub>-NH<sub>3</sub>-driven cases when we could robustly define the track of the cluster evolution, the cluster growth was continuous and near linear for cluster sizes up to 3 nm, suggesting co-condensation of H<sub>2</sub>SO<sub>4</sub> and NH<sub>3</sub> as the sole growth mechanism. This does not exclude the possibility that organics could also participate in the growth process in Hyytiälä on other days.

In addition, we noticed that there was a mechanism driving the IIN, and HOMs are most likely to be the responsible species, although H<sub>2</sub>SO<sub>4</sub> and NH<sub>3</sub> might also participate in this mechanism. Such a mechanism was responsible for

at least 35 IIN events during the measurement days and is expected to be the prevailing one in higher-temperature seasons.

The contribution of IIN to the total rates of NPF differs between events driven by H<sub>2</sub>SO<sub>4</sub>-NH<sub>3</sub> and by HOMs. IIN plays a bigger role in HOM-driven events, likely due to a relatively stronger stabilizing effect of ions. Since the production of HOMs and H<sub>2</sub>SO<sub>4</sub> are strongly modulated by solar radiation and/or temperature, seasonal variation in IIN can be expected, not only in terms of frequency but also in terms of the underlying mechanisms and hence in terms of the enhancing effect of ions. This information should be considered in aerosol formation modeling in future works.

*Data availability.* The processed APi-TOF data, as well as other relevant parameters, are available at: <https://doi.org/10.5281/zenodo.1408617> (Chao, 2018). For the raw mass spectrometer data, please contact the first author via email: [chao.yan@helsinki.fi](mailto:chao.yan@helsinki.fi)

*Author contributions.* CY and LD wrote the paper. CY, LD, and CR analyzed the main datasets. TJ, SS, HJ, and UM collected the data. All listed coauthors contributed to the manuscript by useful scientific discussions or comments.

*Competing interests.* The authors declare that they have no conflict of interest.

*Acknowledgements.* This work was partially funded by the Academy of Finland (1251427, 1139656, 296628, 306853, Finnish centre of excellence 1141135), the EC Seventh Framework Program and European Union's Horizon 2020 program (Marie Curie ITN no. 316662 "CLOUD-TRAIN", no. 656994 "Nano-CAVA",

no. 227463 “ATMNUCLE”, no. 638703 “COALA”, no. 714621 “GASPARCON”, and no. 742206 “ATM-GTP”), and the European Regional Development Fund project “MOBTT42”. We thank the tofTools team for providing tools for mass spectrometry analysis.

Edited by: Gordon McFiggans

Reviewed by: two anonymous referees

## References

- Aalto, P., Hämeri, K., Becker, E., Weber, R., Salm, J., Mäkelä, J. M., Hoell, C., O’Dowd, C. D., Karlsson, H., and Hansson, H. C.: Physical characterization of aerosol particles during nucleation events, *Tellus B*, 53, 344–358, 2001.
- Almeida, J., Schobesberger, S., Kuerten, A., Ortega, I. K., Kupiainen-Maatta, O., Praplan, A. P., Adamov, A., Amorim, A., Bianchi, F., Breitenlechner, M., David, A., Dommen, J., Donahue, N. M., Downard, A., Dunne, E., Duplissy, J., Ehrhart, S., Flagan, R. C., Franchin, A., Guida, R., Hakala, J., Hansel, A., Heinritzi, M., Henschel, H., Jokinen, T., Junninen, H., Kajos, M., Kangasluoma, J., Keskinen, H., Kupc, A., Kürten, T., Kvashin, A. N., Laaksonen, A., Lehtipalo, K., Leiminger, M., Leppä, J., Loukonen, V., Makhmutov, V., Mathot, S., McGrath, M. J., Nieminen, T., Olenius, T., Onnela, A., Petaja, T., Riccobono, F., Riipinen, I., Rissanen, M., Rondo, L., Ruuskanen, T., Santos, F. D., Sarnela, N., Schallhart, S., Schnitzhofer, R., Seinfeld, J. H., Simon, M., Sipila, M., Stozhkov, Y., Stratmann, F., Tome, A., Troestl, J., Tsagkogeorgas, G., Vaattovaara, P., Viisanen, Y., Virtanen, A., Vrtala, A., Wagner, P. E., Weingartner, E., Wex, H., Williamson, C., Wimmer, D., Ye, P., Yli-Juuti, T., Carslaw, K. S., Kulmala, M., Curtius, J., Baltensperger, U., Worsnop, D. R., Vehkamäki, H., and Kirkby, J.: Molecular understanding of sulphuric acid-amine particle nucleation in the atmosphere, *Nature*, 502, 359–363, <https://doi.org/10.1038/nature12663>, 2013.
- Asmi, E., Sipilä, M., Manninen, H. E., Vanhanen, J., Lehtipalo, K., Gagné, S., Neitola, K., Mirme, A., Mirme, S., Tamm, E., Uin, J., Komsaare, K., Attoui, M., and Kulmala, M.: Results of the first air ion spectrometer calibration and intercomparison workshop, *Atmos. Chem. Phys.*, 9, 141–154, <https://doi.org/10.5194/acp-9-141-2009>, 2009.
- Bianchi, F., Tröstl, J., Junninen, H., Frege, C., Henne, S., Hoyle, C. R., Molteni, U., Herrmann, E., Adamov, A., Bukowiecki, N., Chen, X., Duplissy, J., Gysel, M., Hutterli, M., Kangasluoma, J., Kontkanen, J., Kürten, A., Manninen, H. E., Münch, S., Peräkylä, O., Petäjä, T., Rondo, L., Williamson, C., Weingartner, E., Curtius, J., Worsnop, D. R., Kulmala, M., Dommen, J., and Baltensperger, U.: New particle formation in the free troposphere: A question of chemistry and timing, *Science*, 352, 1109–1112, 2016.
- Bianchi, F., Garmash, O., He, X., Yan, C., Iyer, S., Rosendahl, I., Xu, Z., Rissanen, M. P., Riva, M., Taipale, R., Sarnela, N., Petäjä, T., Worsnop, D. R., Kulmala, M., Ehn, M., and Junninen, H.: The role of highly oxygenated molecules (HOMs) in determining the composition of ambient ions in the boreal forest, *Atmos. Chem. Phys.*, 17, 13819–13831, <https://doi.org/10.5194/acp-17-13819-2017>, 2017.
- Chao, Y.: The role of H<sub>2</sub>SO<sub>4</sub>-NH<sub>3</sub> anion clusters in ion-induced aerosol nucleation mechanisms in the boreal forest, available at: <https://zenodo.org/record/1408617>, 2018.
- Dada, L., Paasonen, P., Nieminen, T., Buenrostro Mazon, S., Kontkanen, J., Peräkylä, O., Lehtipalo, K., Hussein, T., Petäjä, T., Kerminen, V.-M., Bäck, J., and Kulmala, M.: Long-term analysis of clear-sky new particle formation events and non-events in Hyytiälä, *Atmos. Chem. Phys.*, 17, 6227–6241, <https://doi.org/10.5194/acp-17-6227-2017>, 2017.
- Dunne, E. M., Gordon, H., Kurten, A., Almeida, J., Duplissy, J., Williamson, C., Ortega, I. K., Pringle, K. J., Adamov, A., Baltensperger, U., Barnet, P., Benduhn, F., Bianchi, F., Breitenlechner, M., Clarke, A., Curtius, J., Dommen, J., Donahue, N. M., Ehrhart, S., Flagan, R. C., Franchin, A., Guida, R., Hakala, J., Hansel, A., Heinritzi, M., Jokinen, T., Kangasluoma, J., Kirkby, J., Kulmala, M., Kupc, A., Lawler, M. J., Lehtipalo, K., Makhmutov, V., Mann, G., Mathot, S., Merikanto, J., Miettinen, P., Nenes, A., Onnela, A., Rap, A., Reddington, C. L., Riccobono, F., Richards, N. A., Rissanen, M. P., Rondo, L., Sarnela, N., Schobesberger, S., Sengupta, K., Simon, M., Sipila, M., Smith, J. N., Stozhkov, Y., Tome, A., Troestl, J., Wagner, P. E., Wimmer, D., Winkler, P. M., Worsnop, D. R., and Carslaw, K. S.: Global atmospheric particle formation from CERN CLOUD measurements, *Science*, 354, 1119–1124, <https://doi.org/10.1126/science.aaf2649>, 2016.
- Eisele, F., Lovejoy, E., Kosciuch, E., Moore, K., Mauldin, R., Smith, J., McMurry, P., and Iida, K.: Negative atmospheric ions and their potential role in ion-induced nucleation, *J. Geophys. Res.-Atmos.*, 111, 2006.
- Ehn, M., Junninen, H., Petäjä, T., Kurtén, T., Kerminen, V.-M., Schobesberger, S., Manninen, H. E., Ortega, I. K., Vehkamäki, H., Kulmala, M., and Worsnop, D. R.: Composition and temporal behavior of ambient ions in the boreal forest, *Atmos. Chem. Phys.*, 10, 8513–8530, <https://doi.org/10.5194/acp-10-8513-2010>, 2010.
- Ehn, M., Junninen, H., Schobesberger, S., Manninen, H. E., Franchin, A., Sipilä, M., Petaja, T., Kerminen, V. M., Tammet, H., Mirme, A., Mirme, S., Horrak, U., Kulmala, M., and Worsnop, D. R.: An Instrumental Comparison of Mobility and Mass Measurements of Atmospheric Small Ions, *Aerosol Sci. Tech.*, 45, 522–532, <https://doi.org/10.1080/02786826.2010.547890>, 2011.
- Ehn, M., Kleist, E., Junninen, H., Petäjä, T., Lönn, G., Schobesberger, S., Dal Maso, M., Trimborn, A., Kulmala, M., Worsnop, D. R., Wahner, A., Wildt, J., and Mentel, Th. F.: Gas phase formation of extremely oxidized pinene reaction products in chamber and ambient air, *Atmos. Chem. Phys.*, 12, 5113–5127, <https://doi.org/10.5194/acp-12-5113-2012>, 2012.
- Ehn, M., Thornton, J. A., Kleist, E., Sipilä, M., Junninen, H., Pullinen, I., Springer, M., Rubach, F., Tillmann, R., Lee, B., Lopez-Hilfiker, F., Andres, S. Y., Acir, I. H., Rissanen, M., Jokinen, T., Schobesberger, S., Kangasluoma, J., Kontkanen, J., Nieminen, T., Kürten, T., Nielsen, L. B., Jorgensen, S., Kjaergaard, H. G., Canagaratna, M., Dal Maso, M., Berndt, T., Petaja, T., Wahner, A., Kerminen, V. M., Kulmala, M., Worsnop, D. R., Wildt, J., and Mentel, T. F.: A large source of low-volatility secondary organic aerosol, *Nature*, 506, 476–480, <https://doi.org/10.1038/nature13032>, 2014.

- Franchin, A., Ehrhart, S., Leppä, J., Nieminen, T., Gagné, S., Schobesberger, S., Wimmer, D., Duplissy, J., Riccobono, F., Dunne, E. M., Rondo, L., Downard, A., Bianchi, F., Kupc, A., Tsigogeorgas, G., Lehtipalo, K., Manninen, H. E., Almeida, J., Amorim, A., Wagner, P. E., Hansel, A., Kirkby, J., Kürten, A., Donahue, N. M., Makhmutov, V., Mathot, S., Metzger, A., Petäjä, T., Schnitzhofer, R., Sipilä, M., Stozhkov, Y., Tomé, A., Kerminen, V.-M., Carslaw, K., Curtius, J., Baltensperger, U., and Kulmala, M.: Experimental investigation of ion-ion recombination under atmospheric conditions, *Atmos. Chem. Phys.*, 15, 7203–7216, <https://doi.org/10.5194/acp-15-7203-2015>, 2015.
- Frege, C., Ortega, I. K., Rissanen, M. P., Praplan, A. P., Steiner, G., Heinritzi, M., Ahonen, L., Amorim, A., Bernhammer, A.-K., Bianchi, F., Brilke, S., Breitenlechner, M., Dada, L., Dias, A., Duplissy, J., Ehrhart, S., El-Haddad, I., Fischer, L., Fuchs, C., Garmash, O., Gonin, M., Hansel, A., Hoyle, C. R., Jokinen, T., Junninen, H., Kirkby, J., Kürten, A., Lehtipalo, K., Leiminger, M., Mauldin, R. L., Molteni, U., Nichman, L., Petäjä, T., Sarnela, N., Schobesberger, S., Simon, M., Sipilä, M., Stolzenburg, D., Tomé, A., Vogel, A. L., Wagner, A. C., Wagner, R., Xiao, M., Yan, C., Ye, P., Curtius, J., Donahue, N. M., Flagan, R. C., Kulmala, M., Worsnop, D. R., Winkler, P. M., Dommen, J., and Baltensperger, U.: Influence of temperature on the molecular composition of ions and charged clusters during pure biogenic nucleation, *Atmos. Chem. Phys.*, 18, 65–79, <https://doi.org/10.5194/acp-18-65-2018>, 2018.
- Gordon, H., Kirkby, J., Baltensperger, U., Bianchi, F., Breitenlechner, M., Curtius, J., Dias, A., Dommen, J., Donahue, N. M., Dunne, E. M., Duplissy, J., Ehrhart, S., Flagan, R. C., Frege, C., Fuchs, C., Hansel, A., Hoyle, C. R., Kulmala, M., Kürten, A., Lehtipalo, K., Makhmutov, V., Molteni, U., Rissanen, M. P., Stozhkov, Y., Tröstl, J., Tsigogeorgas, G., Wagner, R., Williamson, C., Wimmer, D., Winkler, P. M., Yan, C., and Carslaw, K. S.: Causes and importance of new particle formation in the present-day and preindustrial atmospheres, *J. Geophys. Res.-Atmos.*, 122, 8739–8760, 2017.
- Guo, S., Hu, M., Zamora, M. L., Peng, J., Shang, D., Zheng, J., Du, Z., Wu, Z., Shao, M., Zeng, L., Molina, M. J., and Zhang, R.: Elucidating severe urban haze formation in China, *P. Natl. Acad. Sci. USA*, 111, 17373–17378, <https://doi.org/10.1073/pnas.1419604111>, 2014.
- Hari, P. and Kulmala, M.: Station for measuring ecosystem-atmosphere relations, *Bor. Environ. Res.*, 10, 315–322, 2005.
- Heal, M., Kumar, P., and Harrison, R.: Particles, air quality, policy and health, *Chem. Soc. Rev.*, 41, 6606–6630, 2012.
- Hirsikko, A., Laakso, L., Hörra, U., Aalto, P. P., Kerminen, V. M., and Kulmala, M.: Annual and size dependent variation of growth rates and ion concentrations in boreal forest, *Boreal Environ. Res.*, 10, 357–369, 2005.
- Hirsikko, A., Nieminen, T., Gagné, S., Lehtipalo, K., Manninen, H. E., Ehn, M., Hörrak, U., Kerminen, V.-M., Laakso, L., McMurry, P. H., Mirme, A., Mirme, S., Petäjä, T., Tammet, H., Vakkari, V., Vana, M., and Kulmala, M.: Atmospheric ions and nucleation: a review of observations, *Atmos. Chem. Phys.*, 11, 767–798, <https://doi.org/10.5194/acp-11-767-2011>, 2011.
- Hoppel, W. A.: Ion-aerosol attachment coefficients, ion depletion, and the charge distribution on aerosols, *J. Geophys. Res.*, 90, 5917–5923, 1985.
- Iida, K., Stolzenburg, M., McMurry, P., Dunn, M. J., Smith, J. N., Eisele, F., and Keady, P.: Contribution of ion-induced nucleation to new particle formation: Methodology and its application to atmospheric observations in Boulder, Colorado, *J. Geophys. Res.-Atmos.*, 111, D23201, <https://doi.org/10.1029/2006JD007167>, 2006.
- Jokinen, T., Sipilä, M., Junninen, H., Ehn, M., Lönn, G., Hakala, J., Petäjä, T., Mauldin III, R. L., Kulmala, M., and Worsnop, D. R.: Atmospheric sulphuric acid and neutral cluster measurements using CI-API-TOF, *Atmos. Chem. Phys.*, 12, 4117–4125, <https://doi.org/10.5194/acp-12-4117-2012>, 2012.
- Junninen, H., Ehn, M., Petäjä, T., Luosujärvi, L., Kotiaho, T., Koski, R., Rohner, U., Gonin, M., Fuhrer, K., Kulmala, M., and Worsnop, D. R.: A high-resolution mass spectrometer to measure atmospheric ion composition, *Atmos. Meas. Tech.*, 3, 1039–1053, <https://doi.org/10.5194/amt-3-1039-2010>, 2010.
- Kerminen, V.-M., Paramonov, M., Anttila, T., Riipinen, I., Fountoukis, C., Korhonen, H., Asmi, E., Laakso, L., Lihavainen, H., Swietlicki, E., Svenningsson, B., Asmi, A., Pandis, S. N., Kulmala, M., and Petäjä, T.: Cloud condensation nuclei production associated with atmospheric nucleation: a synthesis based on existing literature and new results, *Atmos. Chem. Phys.*, 12, 12037–12059, <https://doi.org/10.5194/acp-12-12037-2012>, 2012.
- Kirkby, J., Curtius, J., Almeida, J., Dunne, E., Duplissy, J., Ehrhart, S., Franchin, A., Gagné, S., Ickes, L., Kürten, A., Kupc, A., Metzger, A., Riccobono, F., Rondo, L., Schobesberger, S., Tsigogeorgas, G., Wimmer, D., Amorim, A., Bianchi, F., Breitenlechner, M., David, A., Dommen, J., Downard, A., Ehn, M., Flagan, R. C., Haider, S., Hansel, A., Hauser, D., Jud, W., Junninen, H., Kreissl, F., Kvashin, A., Laaksonen, A., Lehtipalo, K., Lima, J., Lovejoy, E. R., Makhmutov, V., Mathot, S., Mikkilä, J., Minginette, P., Mogo, S., Nieminen, T., Onnela, A., Pereira, P., Petäjä, T., Schnitzhofer, R., Seinfeld, J. H., Sipilä, M., Stozhkov, Y., Stratmann, F., Tomé, A., Vanhanen, J., Viisanen, Y., Vrtala, A., Wagner, P. E., Walther, H., Weingartner, E., Wex, H., Winkler, P. M., Carslaw, K. S., Worsnop, D. R., Baltensperger, U., and Kulmala, M.: Role of sulphuric acid, ammonia and galactic cosmic rays in atmospheric aerosol nucleation, *Nature*, 476, 429–433, <https://doi.org/10.1038/nature10343>, 2011.
- Kirkby, J., Duplissy, J., Sengupta, K., Frege, C., Gordon, H., Williamson, C., Heinritzi, M., Simon, M., Yan, C., Almeida, J., Tröstl, J., Nieminen, T., Ortega, I. K., Wagner, R., Adamov, A., Amorim, A., Bernhammer, A.-K., Bianchi, F., Breitenlechner, M., Brilke, S., Chen, X., Craven, J., Dias, A., Ehrhart, S., Flagan, R. C., Franchin, A., Fuchs, C., Guida, R., Hakala, J., Hoyle, C. R., Jokinen, T., Junninen, H., Kangasluoma, J., Kim, J., Krapf, M., Kürten, A., Laaksonen, A., Lehtipalo, K., Makhmutov, V., Mathot, S., Molteni, U., Onnela, A., Peräkylä, O., Piel, F., Petäjä, T., Praplan, A. P., Pringle, K., Rap, A., Richards, N. A. D., Riipinen, I., Rissanen, M. P., Rondo, L., Sarnela, N., Schobesberger, S., Scott, C. E., Seinfeld, J. H., Sipilä, M., Steiner, G., Stozhkov, Y., Stratmann, F., Tomé, A., Virtanen, A., Vogel, A. L., Wagner, A. C., Wagner, P. E., Weingartner, E., Wimmer, D., Winkler, P. M., Ye, P., Zhang, X., Hansel, A., Dommen, J., Donahue, N. M., Worsnop, D. R., Baltensperger, U., Kulmala, M., Carslaw, K. S., and Curtius, J.: Ion-induced nucleation of pure biogenic particles, *Nature*, 533, 521–526, <https://doi.org/10.1038/nature17953>, 2016.

- Kontkanen, J., Lehtinen, K. E. J., Nieminen, T., Manninen, H. E., Lehtipalo, K., Kerminen, V.-M., and Kulmala, M.: Estimating the contribution of ion-ion recombination to sub-2 nm cluster concentrations from atmospheric measurements, *Atmos. Chem. Phys.*, 13, 11391–11401, <https://doi.org/10.5194/acp-13-11391-2013>, 2013.
- Kuang, C., Riipinen, I., Sihto, S.-L., Kulmala, M., McCormick, A. V., and McMurry, P. H.: An improved criterion for new particle formation in diverse atmospheric environments, *Atmos. Chem. Phys.*, 10, 8469–8480, <https://doi.org/10.5194/acp-10-8469-2010>, 2010.
- Kulmala, M., Maso, M. D., Mäkelä, J. M., Pirjola, L., Väkevä, M., Aalto, P., Miikkulainen, P., Hämeri, K., and O'Dowd, C. D.: On the formation, growth and composition of nucleation mode particles, *Tellus B*, 53, 479–490, 2001.
- Kulmala, M., Vehkamäki, H., Petäjä, T., Dal Maso, M., Lauri, A., Kerminen, V.-M., Birmili, W., and McMurry, P. H.: Formation and growth rates of ultrafine atmospheric particles: a review of observations, *J. Aerosol Sci.*, 35, 143–176, 2004.
- Kulmala, M., Petaja, T., Nieminen, T., Sipila, M., Manninen, H. E., Lehtipalo, K., Dal Maso, M., Aalto, P. P., Junninen, H., Paasonen, P., Riipinen, I., Lehtinen, K. E., Laaksonen, A., and Kerminen, V. M.: Measurement of the nucleation of atmospheric aerosol particles, *Nat. Protocol.*, 7, 1651–1667, <https://doi.org/10.1038/nprot.2012.091>, 2012.
- Kulmala, M., Kontkanen, J., Junninen, H., Lehtipalo, K., Manninen, H. E., Nieminen, T., Petäjä, T., Sipilä, M., Schobesberger, S., Rantala, P., Franchin, A., Jokinen, T., Järvinen, E., Äijälä, M., Kangasluoma, J., Hakala, J., Aalto, P. P., Paasonen, P., Mikkilä, J., Vanhanen, J., Aalto, J., Hakola, H., Makkonen, U., Ruuskanen, T., Mauldin, R. L., Duplissy, J., Vehkamäki, H., Bäck, J., Kortelainen, A., Riipinen, I., Kurtén, T., Johnston, M. V., Smith, J. N., Ehn, M., Mentel, T. F., Lehtinen, K. E. J., Laaksonen, A., Kerminen, V.-M., and Worsnop, D. R.: Direct Observations of Atmospheric Aerosol Nucleation, *Science*, 339, 943–946, <https://doi.org/10.1126/science.1227385>, 2013.
- Kürten, A., Bianchi, F., Almeida, J., Kupiainen-Määttä, O., Dunne, E. M., Duplissy, J., Williamson, C., Barmet, P., Breitenlechner, M., Dommen, J., Donahue, N. M., Flagan, R. C., Franchin, A., Gordon, H., Hakala, J., Hansel, A., Heinritzi, M., Ickes, L., Jokinen, T., Kangasluoma, J., Kim, J., Kirkby, J., Kupc, A., Lehtipalo, K., Leiminger, M., Makhmutov, V., Onnela, A., Ortega, I. K., Petäjä, T., Praplan, A. P., Riccobono, F., Rissanen, M. P., Rondo, L., Schnitzhofer, R., Schobesberger, S., Smith, J. N., Steiner, G., Stozhkov, Y., Tomé, A., Tröstl, J., Tsagkogeorgas, G., Wagner, P. E., Wimmer, D., Ye, P., Baltensperger, U., Carlsaw, K., Kulmala, M., and Curtius, J.: Experimental particle formation rates spanning tropospheric sulfuric acid and ammonia abundances, ion production rates, and temperatures, *J. Geophys. Res.-Atmos.*, 121, 12377–12400, <https://doi.org/10.1002/2015jd023908>, 2016.
- Lovejoy, E., Curtius, J., and Froyd, K.: Atmospheric ion-induced nucleation of sulfuric acid and water (1984–2012), *J. Geophys. Res.-Atmos.*, 109, 109, D08204, [doi:10.1029/2003JD004460](https://doi.org/10.1029/2003JD004460), 2004.
- Makkonen, U., Virkkula, A., Hellen, H., Hemmila, M., Sund, J., Aijala, M., Ehn, M., Junninen, H., Keronen, P., Petaja, T., Worsnop, D. R., Kulmala, M., and Hakola, H.: Semi-continuous gas and inorganic aerosol measurements at a boreal forest site: seasonal and diurnal cycles of NH<sub>3</sub>, HONO and HNO<sub>3</sub>, *Boreal Environ. Res.*, 19, 311–328, 2014.
- Manninen, H. E., Nieminen, T., Asmi, E., Gagné, S., Häkkinen, S., Lehtipalo, K., Aalto, P., Vana, M., Mirme, A., Mirme, S., Hörrak, U., Plass-Dülmer, C., Stange, G., Kiss, G., Hoffer, A., Töro, N., Moerman, M., Henzing, B., de Leeuw, G., Brinkenberg, M., Kouvarakis, G. N., Bougiatioti, A., Mihalopoulos, N., O'Dowd, C., Ceburnis, D., Arneth, A., Svenningsson, B., Swietlicki, E., Tarozzi, L., Decesari, S., Facchini, M. C., Birmili, W., Sonntag, A., Wiedensohler, A., Boulon, J., Sellegri, K., Laj, P., Gysel, M., Bukowiecki, N., Weingartner, E., Wehrle, G., Laaksonen, A., Hamed, A., Joutsensaari, J., Petäjä, T., Kerminen, V.-M., and Kulmala, M.: EUCAARI ion spectrometer measurements at 12 European sites – analysis of new particle formation events, *Atmos. Chem. Phys.*, 10, 7907–7927, <https://doi.org/10.5194/acp-10-7907-2010>, 2010.
- McMurry, P. H., Fink, M., Sakurai, H., Stolzenburg, M. R., Mauldin, R. L., Smith, J., Eisele, F., Moore, K., Sjostedt, S., and Tanner, D.: A criterion for new particle formation in the sulfur-rich Atlanta atmosphere, *J. Geophys. Res.-Atmos.*, 110, 2935–2948, 2005.
- Merikanto, J., Spracklen, D. V., Mann, G. W., Pickering, S. J., and Carslaw, K. S.: Impact of nucleation on global CCN, *Atmos. Chem. Phys.*, 9, 8601–8616, <https://doi.org/10.5194/acp-9-8601-2009>, 2009.
- Mirme, S. and Mirme, A.: The mathematical principles and design of the NAIS – a spectrometer for the measurement of cluster ion and nanometer aerosol size distributions, *Atmos. Meas. Tech.*, 6, 1061–1071, <https://doi.org/10.5194/amt-6-1061-2013>, 2013.
- Riccobono, F., Schobesberger, S., Scott, C. E., Dommen, J., Ortega, I. K., Rondo, L., Almeida, J., Amorim, A., Bianchi, F., Breitenlechner, M., David, A., Downard, A., Dunne, E. M., Duplissy, J., Ehrhart, S., Flagan, R. C., Franchin, A., Hansel, A., Junninen, H., Kajos, M., Keskinen, H., Kupc, A., Kürten, A., Kvashin, A. N., Laaksonen, A., Lehtipalo, K., Makhmutov, V., Mathot, S., Nieminen, T., Onnela, A., Petaja, T., Praplan, A. P., Santos, F. D., Schallhart, S., Seinfeld, J. H., Sipila, M., Spracklen, D. V., Stozhkov, Y., Stratmann, F., Tome, A., Tsagkogeorgas, G., Vaattovaara, P., Viisanen, Y., Virtala, A., Wagner, P. E., Weingartner, E., Wex, H., Wimmer, D., Carlsaw, K. S., Curtius, J., Donahue, N. M., Kirkby, J., Kulmala, M., Worsnop, D. R., and Baltensperger, U.: Oxidation products of biogenic emissions contribute to nucleation of atmospheric particles, *Science*, 344, 717–721, <https://doi.org/10.1126/science.1243527>, 2014.
- Rose, C., Zha, Q., Dada, L., Yan, C., Lehtipalo, K., Junninen, H., Mazon, S. B., Jokinen, T., Sarnela, N., Sipila, M., Petaja, T., Kerminen, V. M., Bianchi, F., and Kulmala, M.: Observations of biogenic ion-induced cluster formation in the atmosphere, *Sci. Adv.*, 4, 5218, <https://doi.org/10.1126/sciadv.aar5218>, 2018.
- Schobesberger, S., Junninen, H., Bianchi, F., Lonn, G., Ehn, M., Lehtipalo, K., Dommen, J., Ehrhart, S., Ortega, I. K., Franchin, A., Nieminen, T., Riccobono, F., Hutterli, M., Duplissy, J., Almeida, J., Amorim, A., Breitenlechner, M., Downard, A. J., Dunne, E. M., Flagan, R. C., Kajos, M., Keskinen, H., Kirkby, J., Kupc, A., Kürten, A., Kürten, T., Laaksonen, A., Mathot, S., Onnela, A., Praplan, A. P., Rondo, L., Santos, F. D., Schallhart, S., Schnitzhofer, R., Sipila, M., Tome, A., Tsagkogeorgas, G., Vehkamäki, H., Wimmer, D., Baltensperger, U., Carlsaw, K. S., Curtius, J., Hansel, A., Petaja, T., Kulmala, M., Donahue,

- N. M., and Worsnop, D. R.: Molecular understanding of atmospheric particle formation from sulfuric acid and large oxidized organic molecules, *P. Natl. Acad. Sci. USA*, 110, 17223–17228, <https://doi.org/10.1073/pnas.1306973110>, 2013.
- Schobesberger, S., Franchin, A., Bianchi, F., Rondo, L., Duplissy, J., Kürten, A., Ortega, I. K., Metzger, A., Schnitzhofer, R., Almeida, J., Amorim, A., Dommen, J., Dunne, E. M., Ehn, M., Gagné, S., Ickes, L., Junninen, H., Hansel, A., Kerminen, V.-M., Kirkby, J., Kupc, A., Laaksonen, A., Lehtipalo, K., Mathot, S., Onnela, A., Petäjä, T., Riccobono, F., Santos, F. D., Sipilä, M., Tomé, A., Tsagkogeorgas, G., Viisanen, Y., Wagner, P. E., Wimmer, D., Curtius, J., Donahue, N. M., Baltensperger, U., Kulmala, M., and Worsnop, D. R.: On the composition of ammonia-sulfuric-acid ion clusters during aerosol particle formation, *Atmos. Chem. Phys.*, 15, 55–78, <https://doi.org/10.5194/acp-15-55-2015>, 2015.
- Stocker, T., Qin, D., Plattner, G., Tignor, M., Allen, S., Boschung, J., Nauels, A., Xia, Y., Bex, B., and Midgley, B.: in: IPCC, 2013, Climate change 2013, The physical science basis. Contribution of working group I to the fifth assessment report of the intergovernmental panel on climate change, 2013.
- Tammet, H. and Kulmala, M.: Simulation tool for atmospheric aerosol nucleation bursts, *J. Aerosol Sci.*, 36, 173–196, 2005.
- Wagner, R., Yan, C., Lehtipalo, K., Duplissy, J., Nieminen, T., Kangasluoma, J., Ahonen, L. R., Dada, L., Kontkanen, J., Manninen, H. E., Dias, A., Amorim, A., Bauer, P. S., Bergen, A., Bernhammer, A.-K., Bianchi, F., Brilke, S., Mazon, S. B., Chen, X., Draper, D. C., Fischer, L., Frege, C., Fuchs, C., Garmash, O., Gordon, H., Hakala, J., Heikkinen, L., Heinritzi, M., Hofbauer, V., Hoyle, C. R., Kirkby, J., Kürten, A., Kvashnin, A. N., Laurila, T., Lawler, M. J., Mai, H., Makhmutov, V., Mauldin III, R. L., Molteni, U., Nichman, L., Nie, W., Ojdanic, A., Onnela, A., Piel, F., Quéléver, L. L. J., Rissanen, M. P., Sarnela, N., Schallhart, S., Sengupta, K., Simon, M., Stolzenburg, D., Stozhkov, Y., Tröstl, J., Viisanen, Y., Vogel, A. L., Wagner, A. C., Xiao, M., Ye, P., Baltensperger, U., Curtius, J., Donahue, N. M., Flagan, R. C., Gallagher, M., Hansel, A., Smith, J. N., Tomé, A., Winkler, P. M., Worsnop, D., Ehn, M., Sipilä, M., Kerminen, V.-M., Petäjä, T., and Kulmala, M.: The role of ions in new particle formation in the CLOUD chamber, *Atmos. Chem. Phys.*, 17, 15181–15197, <https://doi.org/10.5194/acp-17-15181-2017>, 2017.
- Yan, C., Nie, W., äijälä, M., Rissanen, M. P., Canagaratna, M. R., Massoli, P., Junninen, H., Jokinen, T., Sarnela, N., Häme, S. A. K., Schobesberger, S., Canonaco, F., Yao, L., Prévôt, A. S. H., Petäjä, T., Kulmala, M., Sipilä, M., Worsnop, D. R., and Ehn, M.: Source characterization of highly oxidized multifunctional compounds in a boreal forest environment using positive matrix factorization, *Atmos. Chem. Phys.*, 16, 12715–12731, <https://doi.org/10.5194/acp-16-12715-2016>, 2016.